Available online at www.sciencedirect.com
SCIENCE DIRECT
ELSEVIER
Journal of Computational and Applied Mathematics 196 (2006) 523–539
JOURNAL OF COMPUTATIONAL AND APPLIED MATHEMATICS
www.elsevier.com/locate/cam

Marker method for the solution of nonlinear diffusion equations

Jerome L.V. Lewandowski*

Princeton University, Plasma Physics Laboratory, Princeton, NJ 08543, USA

Received 19 February 2005

Abstract

The marker method for the solution of nonlinear diffusion equations is described. The method relies on the definition of a convective field associated with the underlying partial differential equation; the information about the approximate solution is associated with the response of an ensemble of markers to this convective field. Some key aspects of the method, such as the selection of the shape function and the initial loading, are discussed in some detail. Numerical experiments show that the method is accurate in determining the long time behavior of nonlinear diffusion equations. The marker method can be applied to an ensemble of nonlinear dispersive partial differential equations.

Keywords: Marker method; Nonlinear diffusion equations; Particle-in-cell method; Dispersive equations

1. Introduction

Marker methods have been used for a long time in plasma physics to give a numerical solution of purely convective problems such as, for example, the collisionless Vlasov equation [1,6,8,9]. In these methods each marker (or 'super-particle') carries the information associated with a small element of phase space. In the absence of collisions, each phase space element changes its shape but its volume remains constant as a consequence of Liouville's theorem. In conventional marker methods [1,6] collisional effects are introduced perturbatively; in the first step, the collisionless trajectories of the markers are followed in phase space; in the second step, the velocities (and possibly the weights) of the markers are modified such as to account for collisional effects. The method presented in this paper allows for the simultaneous treatment of purely convective effects and diffusive effects.

The method can actually be used to solve a more general set of partial differential equations (PDEs) that are encountered commonly in physical and engineering sciences. In this paper a marker method for the solution of nonlinear diffusion equations is described. As it will become apparent in the next section, the marker method can be generalized to nonlinear, dispersive PDEs such as the Korteweg–de Vries (KdV) [7] and Burgers' equation [2].

The main idea behind the marker method for the solution of a given PDE is to rewrite it as a conservation equation with a generalized convective velocity. In general (even in linear cases), the generalized convective velocity depends on the solution of the PDE itself. Each marker, which carries the information of the solution of the PDE through its weight and its position, is advance in time using a Lagrangian scheme. The generalized convective velocity mentioned

* Fax: +1 609 243 2662.
E-mail address: jlewando@pppl.gov.

0377-0427/$ - see front matter © 2005 Elsevier B.V. All rights reserved.
doi:10.1016/j.cam.2005.10.003

earlier is computed through the information contained in the ensemble of markers (and through the so-called shape function [6]).

The marker method, unlike the finite difference and the finite element methods, does not rely on the concept of a grid (of course one can, if needed, reconstruct the solution on a fixed grid through the collective information associated with the markers). Increased resolution can be achieved in a natural way by locally increasing the number of markers and/or modifying the initial loading of the markers. Unlike the finite difference method, the marker method can be trivially extended to multi-dimensional problems.

The marker method is a grid-free method. Ghoniem and Sherman [5] have developed a grid-free simulation method for diffusion equations; their method is self-adaptive and computational elements move according to local gradients. The grid-free method of Ghoniem and Sherman [5] is based on random walks of a set of markers (Monte Carlo simulation) that simulate a continuum field in a diffusion equation. In contrast, the method presented in this paper is deterministic and does not require random numbers.

This paper is organized as follows: in Section 2, the marker method is described in the context of the solution of a one-dimensional linear diffusion equation. The shape function, which is involved in the evaluation of the approximate solution, is analyzed in some detail in the same section. A numerical example is also presented. The marker method is applied to a nonlinear diffusion equation in Section 3 and numerical results are presented. Concluding remarks are given in Section 4.

2. Marker method

In this section, the basic idea behind the marker method is described through a simple example: the linear diffusion equation. An analysis of the smoothing approximation obtained through the shape function is also discussed. A specific numerical application of the marker method to the case of a one-dimensional linear diffusion equation is given.

2.1. Basic idea

For illustrative purposes, we describe the marker method for one-dimensional problems (as mentioned in the Introduction, the generalization to multi-dimensional problems is straightforward). We consider an ensemble of N markers. Each marker k is defined through its position x_k and its weight W_k. The solution of a given one-dimensional PDE is found by allowing the set $\{(x_k, W_k); k = 1, \ldots, N\}$ to evolve in time according to a generalized nonlinear convective velocity. The generalized convective velocity usually depends on the solution itself and a form of convolution of the approximate solution with a shape function is required.

Consider the one-dimensional diffusion equation

$$\frac{\partial f}{\partial t} = \frac{\partial^2 f}{\partial x^2}, \tag{1}$$

subject to the initial condition $f_0(x) = f(x, 0)$. The main idea behind the marker method is to write Eq. (1) as a (nonlinear) conservation equation

$$\frac{\partial f}{\partial t} + \frac{\partial}{\partial x}(Vf) = 0, \tag{2}$$

where

$$V = -\frac{1}{f}\frac{\partial f}{\partial x}. \tag{3}$$

For clarity, $f(x, t)$ is used to denote the exact solution of Eq. (1) whereas $F(x, t)$ represents its approximation. The function f can be approximated by an ensemble of markers (or 'superparticles') where each marker j has an associated weight, W_j, and a time-dependent position, $x_j(t)$. As in standard particle methods [1,6], such an approximation

can be written in terms of delta functions

$$\widehat{F} = \sum_{j=1}^{N} W_j \delta(x - x_j), \tag{4}$$

where $\delta(x)$ is the usual Kronecker delta function; the hat notation indicates that the representation is singular. For example, $1/\widehat{F}(x,t)$ can be singular in region where $f(x,t)$ is nonzero; furthermore, the ratio of delta functions is not defined. Substituting the discrete representation (4) in Eq. (2) yields the characteristics associated with the generalized velocity V

$$\left.\begin{array}{l} \mathrm{d}x_j/\mathrm{d}t = V(x_j(t), t) \\ x_j(0) = x_{0j} \end{array}\right\} j = 1, \ldots, N. \tag{5}$$

As noted above, $V \propto \partial\widehat{F}/\partial x/\widehat{F}$ is not well defined. As in conventional particle methods [1,6] a smoothed version of $\widehat{F}$ is obtained by taking the convolution of Eq. (4) with a shape function

$$F(x,t) = (S_\varepsilon \star \widehat{F})(x,t) = \sum_{j=1}^{N} W_j S_\varepsilon(x - x_j), \tag{6}$$

where $S_\varepsilon(x) = S(x/\varepsilon)/\varepsilon$ and $\int S\,\mathrm{d}x = 1$; ε is termed the support parameter. Note that the method can be easily generalized to the noninhomogeneous case. For example, given the diffusion equation of

$$\frac{\partial f}{\partial t} = \frac{\partial^2 f}{\partial x^2} + Q(x),$$

one can easily determine the appropriate velocity V as

$$V = -\frac{1}{f}\frac{\partial f}{\partial x} - \frac{1}{f}\int_{-\infty}^{x} Q(x')\,\mathrm{d}x'.$$

Using representation (6) in the trajectory equations, Eq. (5), one gets

$$\frac{\mathrm{d}x_j}{\mathrm{d}t} = -\frac{\sum_{k=1}^{N} W_k S'_\varepsilon(x_j(t) - x_k(t))}{\sum_{k=1}^{N} W_k S_\varepsilon(x_j(t) - x_k(t))}, \tag{7}$$

where a prime denotes a derivative with respect to x and the initial positions are $x_j(0) = x_{0j}$. Note that the weights in Eq. (7) do not vary in time; in particular, if all the weights are initially equal, then all the information about the approximation $F(x,t)$ is contained in the marker positions. The equations of motion (7) can be integrated using standard ordinary differential equation (ODE) techniques, such as the Runge–Kutta method [10], as used in this paper. As it is apparent in Eq. (3) the generalized velocity V can become singular as $f \mapsto 0$. This apparent singularity is also evident in the equations of motion [Eq. (7)]. Note however that the denominator of Eq. (7) does not vanish in practice. To see this, one can write the denominator of Eq. (7) as

$$\sum_{k=1}^{N} W_k S_\varepsilon(x_j(t) - x_k(t)) = W_j S_\varepsilon(0) + \sum_{k\neq j}^{N} W_k S_\varepsilon(x_j(t) - x_k(t)).$$

Although the last term on the right-hand side of the above equation can vanish, the first term does not. Nevertheless, where the solution is small we except the velocity V to be large and the time step of integration must have to be reduced accordingly.

Before considering a numerical illustration of the marker method, several observations are in order. Clearly the accuracy of the marker method depends crucially on the shape function and its support parameter, ε (see next section). The number of markers, the method of integration of the equations of motion, the initial loading of the ensemble $\{(x_k, W_k); k = 1, \ldots, N\}$ and the time step of integration are parameters that also influence the accuracy of the marker method. In some sense, the positions of the markers define a moving grid as far as the approximate solution is concerned.

Of course one can reconstruct the approximate solution F on a fixed grid $\{X_g;\ g=1,\ldots,N_g\}$ at time t by invoking the representation (6):

$$F_g(t)=F(X_g,t)=\sum_{j=1}^{N} W_j S_\varepsilon(X_g-x_j(t)).$$

The marker method can be easily generalized to *nonlinear* dispersive PDEs such as the KdV equation [7] and Burgers' equation [2]. For example, the KdV equation [7]

$$\frac{\partial f}{\partial t}+3\frac{\partial f^2}{\partial x}+\frac{\partial^3 f}{\partial x^3}=0,$$

can be written as a nonlinear conservation equation [Eq. (2)] with a generalized velocity

$$V(x,t)=3f(x,t)+\frac{\partial^2 f(x,t)/\partial x^2}{f(x,t)},$$

as it can be verified by direct substitution. Therefore the marker method is very versatile in its applications, whereas conventional (e.g. finite difference) methods usually require substantial modifications to account for additional nonlinear or dispersive terms, for example. This is illustrated in Section 3 where the marker method is shown to be easily generalized to a highly nonlinear diffusion equation.

2.2. Analysis of the smoothing approximation

As mentioned in the previous section, the accuracy of the marker method depends crucially on the smoothing approximation of the PDEs approximate solution. Therefore it is important to study the impact of the shape function and its support parameter ε on test functions. As it will become apparent below, the accuracy of the smoothing approximation is also related to the initial loading of the markers. The smoothed approximation of the exact solution $f(x)$ is given by

$$F(x)=\sum_{j=1}^{N} W_j S_\varepsilon(x-x_j), \tag{8}$$

where $S_\varepsilon(x)=S(x/\varepsilon)/\varepsilon$ and the shape function $S(x)$ with finite support satisfies the normalization condition

$$\int_{-1}^{1} S(x)\,\mathrm{d}x=1$$

and $S(x)=0$ for $|x|>1$. In some cases, there are advantages in using shape functions with infinite support, in which case the normalization condition is of the form $\int_{-\infty}^{+\infty} S\,\mathrm{d}x=1$. Apart from the actual form of the shape function, there is some freedom in selecting the value of the support parameter ε. However one can estimate an appropriate value for ε based on the following considerations. For illustrative purposes, consider a simulation with N markers that are initially distributed uniformly in the interval $x\in[-L,L]$; therefore, at $t=0$, the average distance between markers is $h=2L/N$. If the support parameter is such that $\varepsilon<h$, then $S_\varepsilon(x_j-x_k)\propto S((x_j-x_k)/\varepsilon)=0$ for all markers $j\neq k$; this implies that the position of each marker will be independent of the positions of the other markers at least at $t=0$. We conclude that the support parameter must be larger than the average distance between markers, at least in the average sense. In addition, the value of ε, which is akin to a grid spacing in the finite difference method, must be chosen such as to accurately resolve the spatial scale length of $f(x)$. In summary, if λ denotes the (known or estimated) spatial scale length of $f(x)$ and h is the average distance between markers, the support parameter, ε, must satisfy the following inequality:

$$h\ll\varepsilon\ll\lambda.$$

There is some freedom in selecting a shape function. Typically one requires some smoothness properties and/or ease of computation (for example, a Gaussian shape function is smoother than a hat shape function, but it is computationally more demanding to evaluate). Below is a set of shape functions that are defined on the interval $[-1, +1]$:

$$S_1(x) = \tfrac{1}{2} \quad \text{(gate function)},$$

$$S_2(x) = 1 - |x| \quad \text{(hat function)},$$

$$S_3(x) = \tfrac{3}{4}(1 - x^2) \quad \text{(quadratic polynomial)},$$

$$S_4(x) = \tfrac{15}{16}(1 - x^2)^2 \quad \text{(quartic polynomial)},$$

$$S_5(x) = \mu(1 - |x|)\mathrm{e}^{-x^2} \quad \text{(hat/Gaussian shape function)},$$

$$S_6(x) = \beta(1 - x^2)^2\mathrm{e}^{-x^2} \quad \text{(quartic polynomial/Gaussian shape function)}, \tag{9}$$

where $\mu = (\sqrt{\pi}\,\mathrm{erf}\,(1) + 1/e - 1)^{-1}$ and $\beta = 2/(\frac{3}{2}\,\mathrm{erf}\,(1) - 1/e)$ are constants of normalization, and $\mathrm{erf}\,(x)$ denotes the error function

$$\mathrm{erf}\,(x) = \frac{2}{\sqrt{\pi}} \int_0^x \mathrm{e}^{-t^2}\,\mathrm{d}t.$$

The second factor that affects the approximation of $f(x)$ is the distribution of the position of the markers and their associated weights. There are two basic approaches to the initialization of the ensemble $\{(x_j, W_j);\ \ j = 1, \ldots, N\}$. In the first approach, the markers are uniformly distributed in space. Using the approximation of

$$\int f(x)\,\mathrm{d}x \approx \sum_j f(x_j)h,$$

where h is the distance between two consecutive markers, and noting that [see Eq. (4)]

$$\int \widehat{F}\,\mathrm{d}x = \sum_j W_j,$$

it follows that

$$W_j = f(x_j)h,\ x_{j+1} - x_j = h.$$

In the second approach, each marker has the same weight, but the spatial distribution of the markers is not uniform. If there are N markers, the marker weight is then $W_j = \sigma/N$, where $\sigma \equiv \int_{-\infty}^{+\infty} f\,\mathrm{d}x$. In order to determine the spatial distribution of the markers, it is convenient to introduce the variable

$$\xi = \frac{\int_{-\infty}^{x} f(x)\,\mathrm{d}x}{\int_{-\infty}^{+\infty} f(x)\,\mathrm{d}x}$$

which, by construction, is a positive-definite quantity in the unit interval. A uniform distribution in ξ, that is $\xi_j = (j - \frac{1}{2})/N\ \ (\forall j)$, yields

$$x_j = g^{-1}\left(\left(\int_{-\infty}^{+\infty} f(x)\,\mathrm{d}x\right)\frac{j - \frac{1}{2}}{N}\right),$$

$$W_j = \frac{\sigma}{N}, \tag{10}$$

where g^{-1} denotes the inverse of $g(x) \equiv \int_{-\infty}^{x} f(x')\,\mathrm{d}x'$. As a numerical illustration, consider the function

$$f(x) = x\mathrm{e}^{-x^2},$$

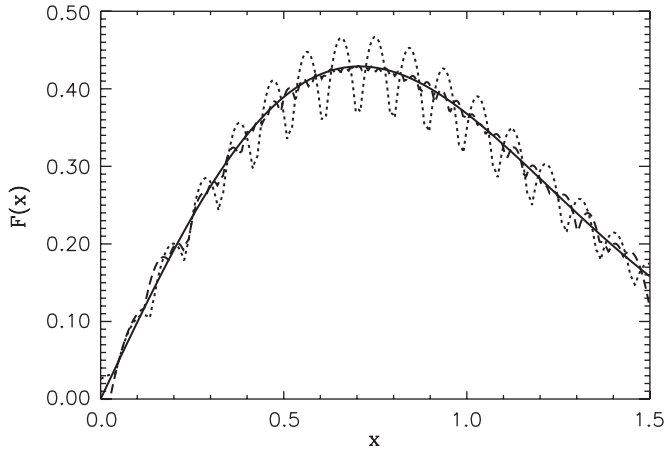

Fig. 1. Approximation of the function $f(x) = x\mathrm{e}^{-x^2}$ (plain line) based on a set of $N = 32$ markers. The dotted (dashed) line is for the case of uniform (nonuniform) spatial loading. The shape function is a quadratic polynomial [$S(x) = S_3(x)$; see Eq. (9)] with parameter $\varepsilon = 0.1$.

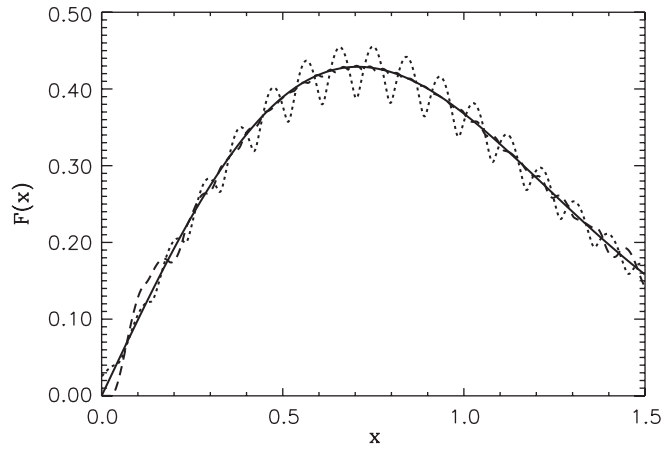

Fig. 2. Approximation of the function $f(x) = x\mathrm{e}^{-x^2}$ (plain line) based on a set of $N = 32$ markers. The dotted (dashed) line is for the case of uniform (nonuniform) spatial loading. The shape function is a quartic polynomial [$S(x) = S_4(x)$; see Eq. (9)] with parameter $\varepsilon = 0.1$.

in the interval $x \in [0, x_0]$, $x_0 > 0$. The initialization based on a set of uniformly distributed x_j yields

$$x_j = (j - 1/2)h,\ W_j = x_j \mathrm{e}^{-x_j^2} h,$$

where $\Delta x = x_0/N$. Alternatively, one can demand that each marker carries an equal weight; following the procedure described in the previous section [Eq. (10)] one obtains

$$x_j = \sqrt{-\ln\left(1 - \frac{j - 1/2}{N}(1 - \mathrm{e}^{-x_0^2})\right)},\ W_j = \frac{1}{N}, \tag{11}$$

Fig. 1 shows the smoothed approximation of $f(x)$ for a uniform spatial loading (dotted line) and a nonuniform spatial loading (dashed line) using a quadratic shape function with support parameter $\varepsilon = 0.1$ for a set of $N = 32$ markers. The plain line represents the exact function. For the same parameters, the quartic shape function, which satisfies $S'(x = \pm 1) = 0$, yields a better approximation (Fig. 2). Further improvement (Fig. 3) can be achieved using the shape function based on a quartic polynomial and a Gaussian function [$S(x) = S_6(x)$; see Eq. (9)]. Of course, in all the above cases, smoother approximations can be obtained by increasing the number of markers N. Another parameter affecting the quality of the approximation is the support parameter, ε. Fig. 4 is the same as Fig. 2 except that the support parameter

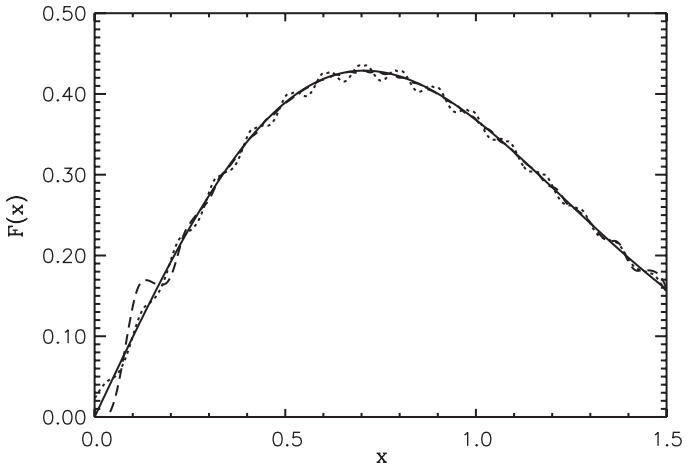

Fig. 3. Approximation of the function $f(x) = x\mathrm{e}^{-x^2}$ (plain line) based on a set of $N = 32$ markers. The dotted (dashed) line is for the case of uniform (nonuniform) spatial loading. The shape function is a based on a quartic polynomial and a Gaussian function [$S(x) = S_6(x)$; see Eq. (9)] with parameter $\varepsilon = 0.1$.

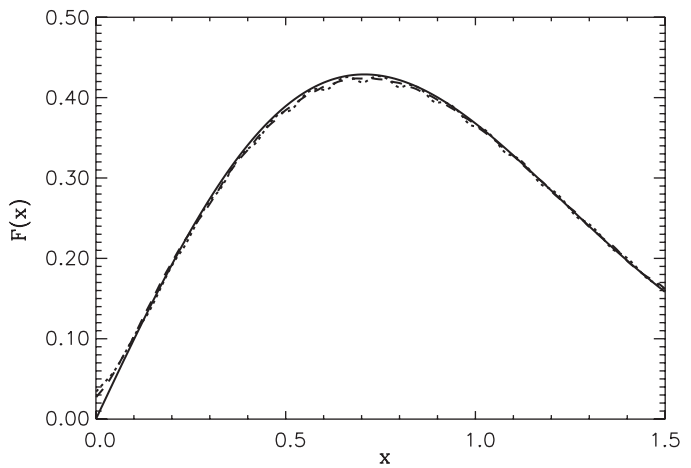

Fig. 4. Approximation of the function $f(x) = x\mathrm{e}^{-x^2}$ (plain line) based on a set of $N = 32$ markers. The dotted (dashed) line is for the case of uniform (nonuniform) spatial loading. The shape function is a quartic polynomial [$S(x) = S_4(x)$; see Eq. (9)] with parameter $\varepsilon = 0.2$.

has been doubled ($\varepsilon = 0.2$). Clearly a much better agreement between the approximated functions and the exact function is found. If the support parameter is further increased the smoothing effect of $S(x)$ becomes too important and the quality of the approximated function degrades.

In the multidimensional case, the markers can be uniformly distributed in space in a straighforward way. A nonuniform spatial loading is however more difficult since the generalization of the quantity ξ mentioned above does not yield a simple algorithm for the marker loading. It is however possible to adopt an alternative approach. For sake of clarity, consider a two-dimensional function $f(x, y)$. For convenience, we introduce the spatial averages of f as

$$\langle f \rangle_x(y) \equiv \int_{-\infty}^{+\infty} f(x', y)\, \mathrm{d}x'$$

and

$$\langle f \rangle_y(x) \equiv \int_{-\infty}^{+\infty} f(x, y')\, \mathrm{d}y'.$$

Instead of a single variable ξ we now define the set (ξ_x, ξ_y) such that

$$\xi_x = \frac{\int_{-\infty}^{x} \langle f \rangle_y(x)\,\mathrm{d}x}{\int_{-\infty}^{+\infty} \langle f \rangle_y(x)\,\mathrm{d}x}$$

and

$$\xi_y = \frac{\int_{-\infty}^{y} \langle f \rangle_x(y)\,\mathrm{d}y}{\int_{-\infty}^{+\infty} \langle f \rangle_x(y)\,\mathrm{d}y}.$$

The procedure for the one-dimensional case can be generalized to a uniform loading in ξ_x and ξ_y; note, however, that the alternative method presented here is not equivalent to the one-dimensional case since the loading in the x and y directions are decoupled.

It it worth noting that the smoothing technique based on Gaussian-like shape functions presented in this section is not unique. In fact it is sometimes justified to formulate shape functions that take into account the underlying PDE to be solved. In that spirit the reader should consult the paper by Chen [3] in which the radial basis function (RBF in short) is described.

2.3. Numerical example for the linear diffusion equation

In this section, we apply the marker method for the diffusion equation, Eq. (1), with initial conditions

$$\left.\begin{aligned} f_0(x) &= 1; \quad |x| \leqslant 1 \\ &= 0; \quad |x| > 1. \end{aligned}\right\} \tag{12}$$

The solution of the diffusion equation, Eq. (1), with initial conditions (12) is easily found using Laplace transforms

$$f(x,t) = \frac{1}{\sqrt{4\pi t}} \int_{-\infty}^{+\infty} f_0(\xi) \exp(-(x-\xi)^2/4t)\,\mathrm{d}\xi = \frac{1}{2}\left[\mathrm{erf}\left(\frac{x+1}{2\sqrt{t}}\right) - \mathrm{erf}\left(\frac{x-1}{2\sqrt{t}}\right)\right],$$

where, as before, $\mathrm{erf}\,(x)$ is the error function with argument x. There is some freedom in the choice of the shape function $S(x)$. Here we have considered 2 shape functions with finite support

$$S_4(x) = \tfrac{15}{16}\,(1-x^2)^2 \quad \text{(quartic polynomial)} \tag{13}$$

and

$$S_7(x) = \alpha(1-x^2)\mathrm{e}^{-x^2} \quad \text{(quadratic polynomial/Gaussian)}, \tag{14}$$

where $\alpha = (1/e + \sqrt{\pi}\mathrm{erf}\,(1)/2)^{-1}$ is a constant of normalization, as well as a shape function with infinite support (superGaussian)

$$S_8(x) = \frac{3/2 - x^2}{\sqrt{\pi}}\,\mathrm{e}^{-x^2}. \tag{15}$$

The equations of motion (7) have been integrated using a second-order Runge–Kutta method [10] with a fixed time step. The approximate solution $F(x,t)$ has been 'reconstructed' on a fixed grid $X_g = -L + (g-1)\Delta X$ for $g = 1, \ldots, N_g$ with grid spacing $\Delta X = 2L/(N_g - 1)$ and on a moving grid defined by the marker positions $\mathbf{x} = \{x_j(t);\ j = 1, \ldots, N\}$. The accuracy of the approximate solution will depend on the support parameter ε. Intuitively, the solution will be oscillatory if ε is too small, whereas $F(x,t)$ will represent a smoothed version of $f(x,t)$ if the support parameter is too large. Figs. 5–7 illustrate this aspect. In these figures, the dotted and plain line represent the approximate and exact solutions, respectively, at $t = 4.0$. The parameters are: $\Delta t = 0.02$, $L = 14.0$, $N_g = 1000$ and the number of markers is $N = 256$. The shape function is the super Gaussian, Eq. (15). Fig. 5 shows the approximate and exact solution for the case of a small support parameter, $\varepsilon = 0.2$. The first-order derivative of the approximate solution is clearly overestimated compared to that of the exact solution; this is due to the fact that a small ε is unable to capture the large scale features associated with $F(x,t)$. On the other hand, $|\partial F/\partial x|$ is too small when the support parameter is too large (Fig. 6). An intermediate value of $\varepsilon = 1.0$ seems to be optimal and a good approximation is obtained with few markers (Fig. 7).

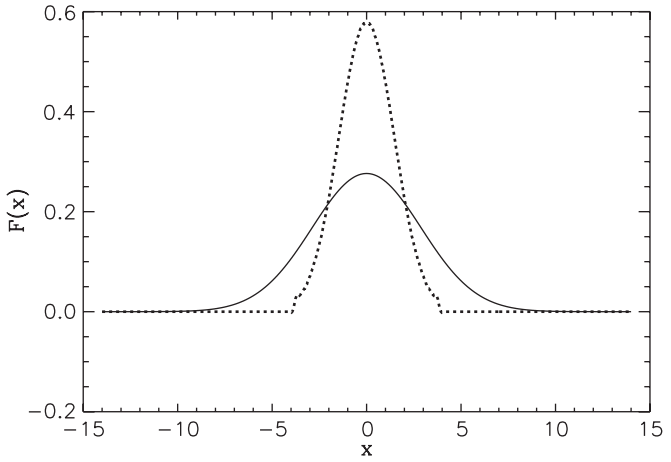

Fig. 5. Exact (plain line) and approximate (dotted line) solutions of the diffusion equation at $t = 4.0$. The initial condition is a square profile, Eq. (12), and the support parameter is $\varepsilon = 0.2$. Other parameters are: $\Delta t = 0.02$, $L = 14.0$, $N_g = 1000$ and $N = 256$.

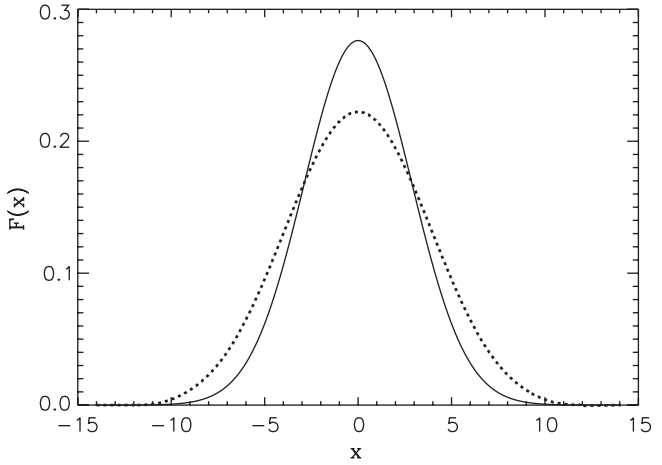

Fig. 6. Same as Fig. 5 but for $\varepsilon = 2.0$.

Figs. 8–13 show the impact of the shape function on the accuracy of the approximate solution at $t = 5.0$ (as before, the plain line represents the exact solution whereas the dotted line is the approximate solution). Figs. 8–10 are for a fixed grid whereas Figs. 11–13 are for a moving grid. The parameters are: $L = 14.0$, $\Delta t = 0.05$, $N_g = 1000$, $N = 256$ and $\varepsilon = 1.0$. Fig. 8 is for the case of a quartic shape function. The formation of wiggles around $x = 0$ is due to a 'clustering effect' in the marker position, as can be seen in Fig. 11 where the same quantities are displayed on a moving grid. In Figs. 11–13 the exact solution has been evaluated on the moving grid using the representation given by Eq. (6). As a result, the way the exact solution is depicted is dependent on the number of markers, the shape function and its support parameter, and the position of the markers at that specific time. The reason for doing so is to highlight the fact that the poor approximate solutions obtained in Figs. 11 and 12 are actually the result of poor representations of F themselves, rather than cumulative errors in the integration of equations of motion. If the representation of F is sufficiently smooth, then much better agreement with the exact solution is found, as it is shown in Fig. 13. Note that the distance between clusters in Fig. 11 is of the order of ε. The use of a Gaussian shape function, Eq. (14), somewhat improves the approximation (Fig. 9). However the clustering effect due to the finite support of $S(x)$ is also apparent in Fig. 12. Figs. 10 and 13 are for the case of a super Gaussian [Eq. (15)]. The clustering effect is absent and the approximate solution is in good agreement with the exact solution. The use of a shape function with finite support

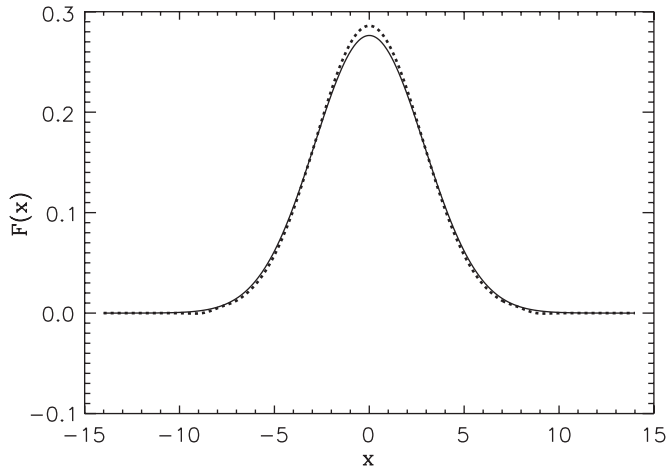

Fig. 7. Same as Fig. 5 but for $\varepsilon = 1.0$.

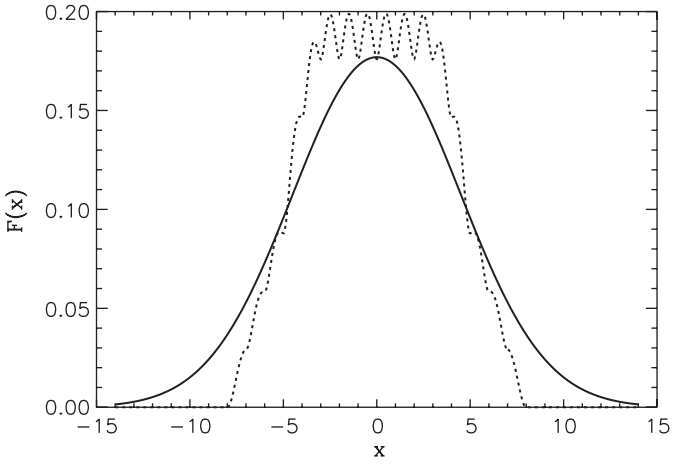

Fig. 8. Exact (plain line) and approximate (dotted line) solutions of the diffusion equation at $t = 5.0$ on a fixed grid for the shape function based on a quartic polynomial, Eq. (13). Other parameters are: $\varepsilon = 1.0$, $\Delta t = 0.05$, $L = 14.0$, $N_g = 1000$ and $N = 256$.

leads to a 'clustering' in the marker position. Note that the distance between clusters is of the order of ε. The same phenomenon is observed when using a shape function based on Eq. (14) as shown in Fig. 9. The use of a shape function based on a super Gaussian, with has infinite support, improves the accuracy of the approximate solution considerably (Fig. 10) because of the absence of clustering (Fig. 13). The impact of finite support shape functions on the accuracy of the approximate solutions can be accessed by monitoring the L^2 norm of the error on a fixed grid

$$E(t) = \left(\Delta X \sum_{g=1}^{N_g} (f(X_g, t) - F(X_g, t))^2 \right)^{1/2}.$$

Fig. 14 shows the above quantity as a function of time for the case of a quartic shape function. The parameters are the same as those of Fig. 8. After an initial decrease in the error norm, E increases almost linearly. A similar behavior is observed for the case of a shape function based on a Gaussian shape function with finite support (Fig. 15). The increase in the error norm can be traced back to the clustering effect depicted in Figs.11 and 12. For the case of a super Gaussian shape function the error norm decreases almost exponentially (Fig. 16).

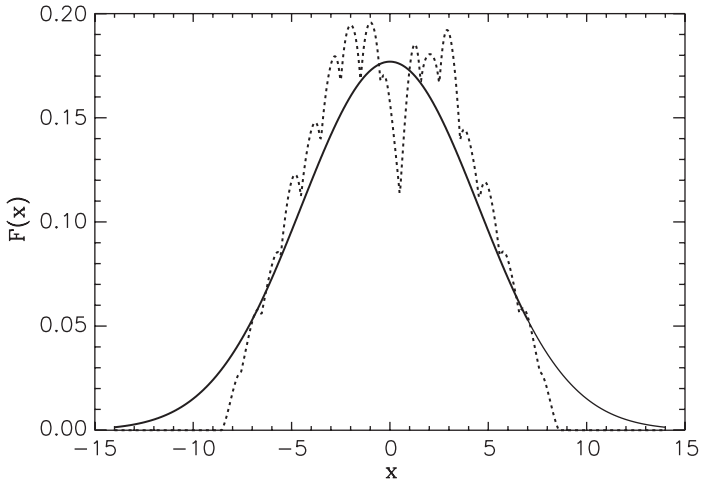

Fig. 9. Same as Fig. 8 but for a Gaussian shape function, Eq. (14).

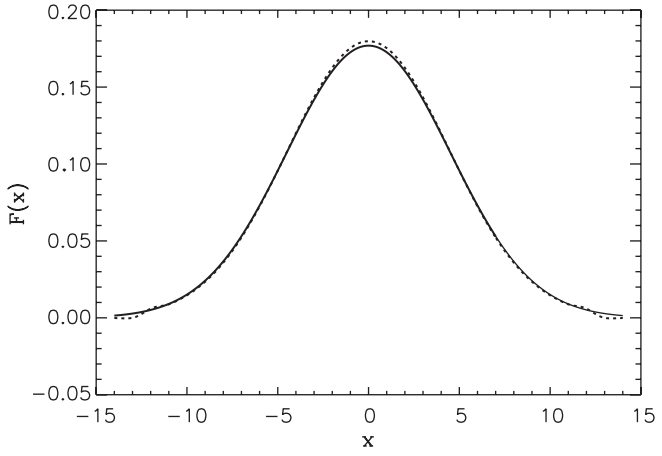

Fig. 10. Same as Fig. 8 but for a super Gaussian shape function, Eq. (15).

Apart from the shape function and the value of the support parameter, the time step and the number of markers N also affect the accuracy of the computed solution. The time step must of course be chosen to ensure stability. Numerical experiments have shown that a time step of

$$\Delta t < \eta\varepsilon^2,$$

where η is a constant of the order of unity, ensure stability. This result is not surprising since an explicit method is used to integrate the equations of motion which, in turn, are derived from a diffusion equation; it is well known that if an explicit (e.g. Euler) integration scheme is used to advance the finite-difference form of Eq. (1) then the time step must satisfy the constraint of

$$\Delta t < \tfrac{1}{2}\,(\Delta x)^2,$$

to ensure stability [4]. Another parameter that impacts the accuracy of the marker method is the number of markers. Of course a larger number of markers yields a better approximation although this implies additional computational work. The relevant parameter is actually the number of markers divided by the support parameter, N/ε; this quantity is a rough measure of the resolution of the marker method (although the optimal value of N/ε can be problem dependent, an average number of markers per ε of 10–15 yield accurate results). We also note that the number of markers is a

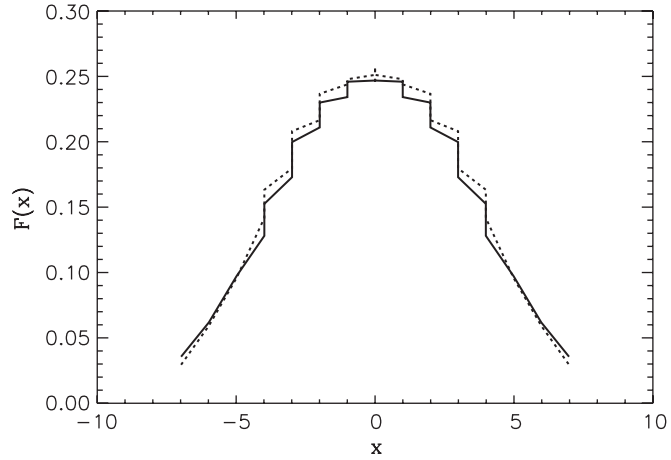

Fig. 11. Exact (plain line) and approximate (dotted line) solutions of the diffusion equation at $t = 5.0$ on a moving grid for the shape function based on a quartic polynomial, Eq. (13). Other parameters are: $\varepsilon = 1.0$, $\Delta t = 0.05$, $L = 14.0$, $N_g = 1000$ and $N = 256$.

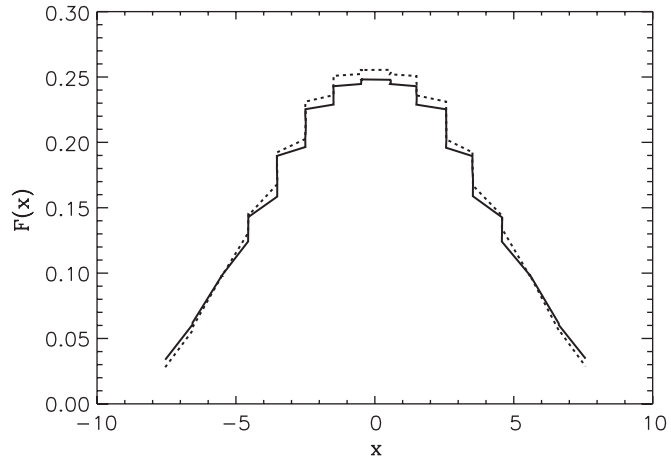

Fig. 12. Same as Fig. 11 but for a Gaussian shape function, Eq. (14).

conserved quantity since the domain of definition of f is the real axis. Although the domain of definition of the original PDE is infinite, the computational domain is finite but increases with time.

2.4. Additional remarks about the marker method

In the previous section the stability of the marker method has been discussed. In particular the time step of integration cannot exceed the classical limit associated with the usual explicit integration schemes. In this section we estimate the accuracy of the marker method. Clearly the shape function, the support parameter, the mean distance between markers and the time step of integration affect the overall accuracy of the method. Note that the convective velocity V is in general a *nonlinear* function of the position of the markers; this is true even if the original PDE is linear (a simple example is the homogeneous heat equation); therefore to determine an exact bound for the error is not straighforward even for a linear PDE. We now return to the discrete approximation of $f(x, t)$ given by Eq. (6). Even if the equation of motions given by Eq. (5) are integrated exactly, the representation (6) is not exact since (a) the support parameter ε is finite; (b) the shape function $S(x)$ is not infinitely smooth; and (c) the mean distance between markers, $h \propto 1/N$, is finite. The approximate solution of Eq. (5) is obtained through an integration of Eq. (7) which depends on the mean

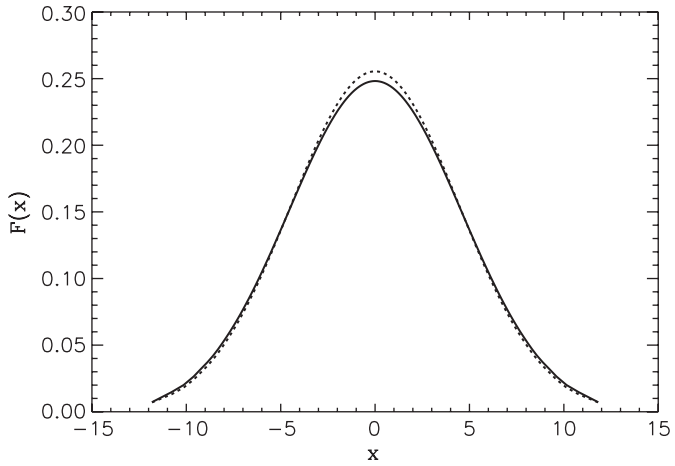

Fig. 13. Same as Fig. 11 but for a super Gaussian shape function, Eq. (15).

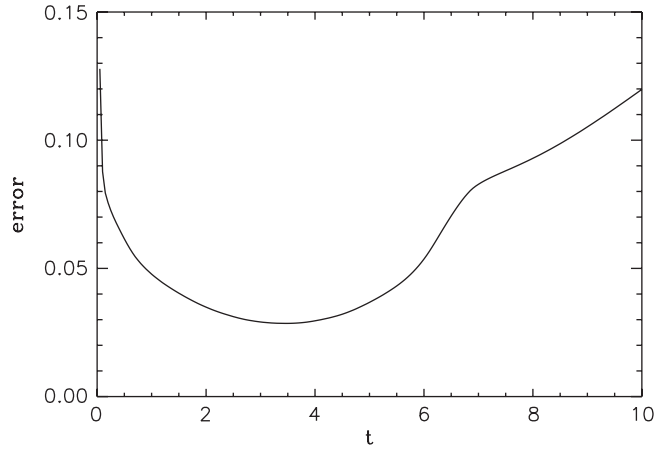

Fig. 14. L^2 norm of the error as a function of time for the case of a quartic shape function, Eq. (13). The parameters are: $\varepsilon = 1.0$, $\Delta t = 0.05$, $L = 14.0$, $N_g = 1000$ and $N = 256$.

distance between markers; therefore we use the notation of $x_j(t)$ to denote the exact solution of the jth equation of motion (5) and $x_j^{(h)}(t)$ to denote its approximation [obtained through an integration of Eq. (7)]. If $f(x,t)$ is the exact solution of the original PDE the error can be defined as

$$e(x,t) \equiv f(x,t) - \sum_{j=1}^{N} W_j S_\varepsilon(x - x_j^{(h)}(t)) \tag{16}$$

which, without loss of generality, can also be written as

$$e(x,t) = f(x,t) - \sum_{j=1}^{N} W_j S_\varepsilon(x - x_j(t)) + \widehat{e}(x,t), \tag{17}$$

where

$$\widehat{e}(x,t) = \sum_{j=1}^{N} W_j \left[S_\varepsilon(x - x_j(t)) - S_\varepsilon(x - x_j^{(h)}(t)) \right]. \tag{18}$$

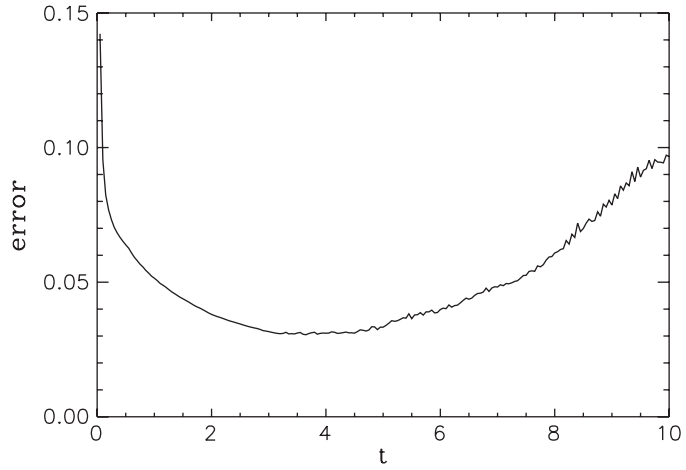

Fig. 15. Same as Fig. 14 but for the case of a gaussian shape function, Eq. (14).

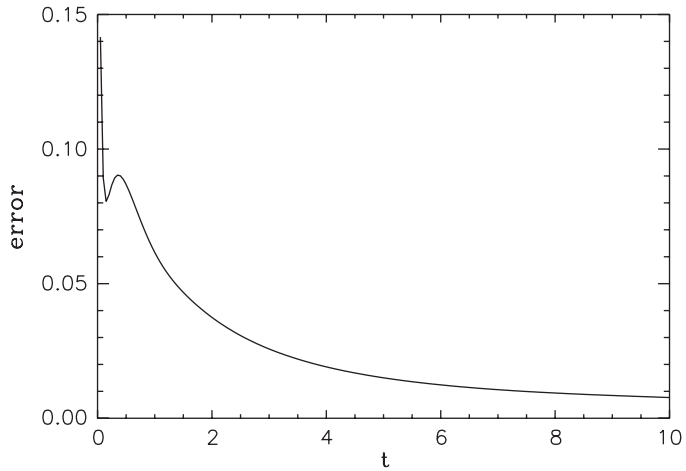

Fig. 16. Same as Fig. 14 but for the case of a super Gaussian shape function, Eq. (15).

Clearly the part of the error associated with $\widehat{e}(x,t)$ is much smaller than the difference $f(x,t)-\sum_{j=1}^{N} W_j S_\varepsilon(x-x_j(t))$ in Eq. (17). The infinite norm of the dominant part of the error can be estimated using the classic analysis for particle methods [see the paper by Raviart [11] and is given by

$$|e|_\infty \sim C(\varepsilon^k + (h/\varepsilon)^M), \tag{19}$$

where C is a constant, M is related to the smoothness of the shape function and k is related to the higher-order vanishing moment of $S(x)$. For a given support parameter ε the error grows with h; since the markers tend to reproduce the dynamics of the (physical) particles, a diffusion process implies that h, and therefore the error, increases in time. For a fixed mean distance h, Eq. (19) shows that an optimal of the support parameter does exist: $\varepsilon_{\text{opt}} = (Mh^M/k)^{1/(k+M)}$. Note that the dependence of the optimal support parameter on k and M is not trivial.

3. Nonlinear diffusion equation

In this section, we apply the marker method to the solution of nonlinear diffusion equations. As in the previous section, we consider the one-dimensional case as the complexity of the algorithm is not affected by the dimensionality

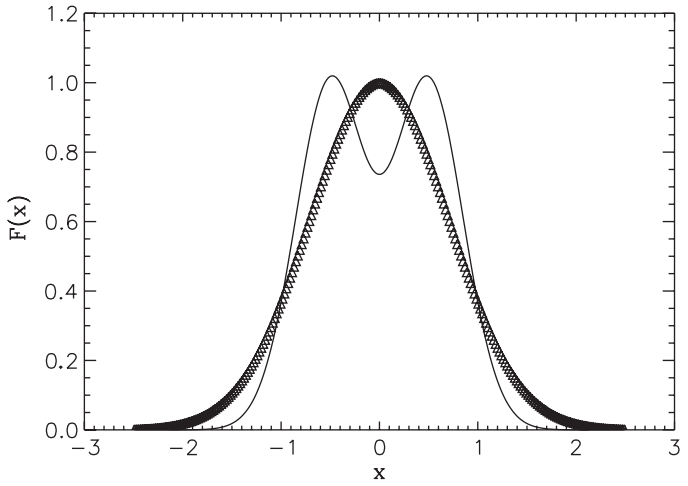

Fig. 17. Steady state solution of the one-dimensional nonlinear diffusion (20) (plain line). The triangles represents the initial position of the markers.

of the problem. The nonlinear diffusion equation is written

$$\frac{\partial f}{\partial t} = \frac{\partial}{\partial x}\left(D\,\frac{\partial f}{\partial x}\right) + Q(x), \tag{20}$$

with a diffusion coefficient of the form $D = D_0 f \mathrm{e}^{-f}$ and a source term

$$Q(x) = -D_0 \mathrm{e}^{-f_\infty}\left[f_\infty\,\frac{\partial^2 f_\infty}{\partial x^2} + (1 - f_\infty)\left(\frac{\partial f_\infty}{\partial x}\right)^2\right]. \tag{21}$$

Here $f_\infty = f_\infty(x)$ denotes the steady state solution of Eq. (20). The nonlinear diffusion Eq. (20) can be written as a conservation equation [Eq. (2)] with a generalized velocity given by

$$V(x,t) = -\frac{D\partial f/\partial x + \widehat{S}(x)}{f}, \tag{22}$$

where

$$\widehat{S}(x) = \int_{-\infty}^{x} Q(x')\,\mathrm{d}x'. \tag{23}$$

The presence of the integral in Eq. (23) can be computationally prohibitive since $S(x)$ is required for every marker at every time step. In order to bypass this difficulty, $S(x)$ has been computed at the beginning of the simulations for a set of fixed grid points; the evaluation of this quantity at the marker position is carried out through a linear interpolation using tabulated values of $S(x)$.

The steady state solution has been taken as

$$f_\infty(x) = \exp(-\alpha(x + x_0)^2) + \exp(-\alpha(x - x_0)^2) \tag{24}$$

and the initial profile is a Gaussian centered at $x = 0$:

$$f_0(x) = f(x,0) = \mathrm{e}^{-x^2}. \tag{25}$$

Fig. 17 shows the steady state solution [Eq. (24)] and the initial profile (triangles) for a set of $N = 256$ markers uniformly distributed in the interval $[-\frac{5}{2}, \frac{5}{2}]$. Other parameters are $\alpha = 4.0$, $x_0 = 0.5$ and $D_0 = 10$; the support parameter has been chosen as $\varepsilon = \sqrt{h}$ where h is the average distance between markers at $t = 0$. The shape function used is a super Gaussian. As in the linear case, the equations of motions have been advanced in time using a second-order Runge–Kutta

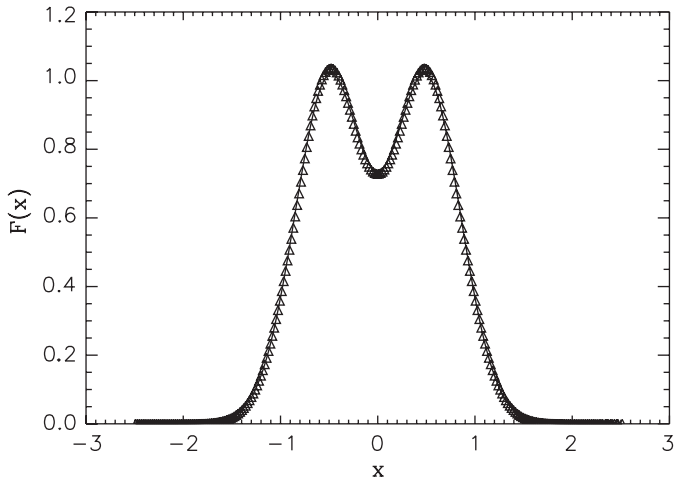

Fig. 18. Steady state solution of the one-dimensional nonlinear diffusion (20) (plain line). The triangles represents the position of the markers at $t = 80$.

integrator [10] with a fixed time step $\Delta t = 0.01$. Fig. 18 shows the steady solution and the approximate solution at the marker positions (triangles) at $t = 80$. We note the excellent agreement between the computed solution and the exact solution. This numerical example highlights one important advantage of the marker method: it is accurate in determining the long-time behavior of highly nonlinear dispersive equations. Further the actual implementation of the algorithm is straightforward and be easily adapted to more complex nonlinear dispersive PDEs.

4. Conclusions

In this paper we have introduced the marker method for the solution of nonlinear partial differential equations. The main idea behind the marker method is to rewrite a given PDE as a conservation equation. A set of markers is then advanced in time (Lagrangian scheme) according to a generalized convective velocity associated with the conservation equation (which itself is an alternative (but exact) form of the original PDE). The information about the approximate solution can be obtained through a convolution of the markers' weights and positions with a shape function. In this paper, we have addressed several aspects of the marker method such as the choice of the shape function and the initial loading of the markers. It has been shown that the method can be used to determine the long time behavior of nonlinear diffusion equation. The main advantages of the marker method are its ease of implementation, flexibility and accuracy. Further, the marker method is of course applicable to PDEs which solutions display one or more shocks since the method is Lagrangian in nature; finite difference methods are often (but not always) not accurate in such situations. Note however that the marker method is suitable for PDEs that involve convective and diffusive terms. Consider for example Burgers' equation [2]

$$\frac{\partial f}{\partial t} + f\,\frac{\partial f}{\partial x} = \mu\,\frac{\partial^2 f}{\partial x^2}, \quad (\mu > 0).$$

Conventional particle methods are well suited when $\mu = 0$; the diffusion term is usually treated perturbatively using a Monte Carlo method. In the marker method, *both* terms are included in the marker dynamics in a *deterministic* way. The marker method has, however, some limitations. One such limitation is that the solution must be positive definite. Although in some problems one can use coordinate trsnaformations to ensure $f \geqslant 0$, this is not always the case.

Of course the marker method cannot handle all nonlinear PDEs (dispersive or not). However the main reasons for employing the marker method (apart from the reasons already mentioned above) for specific problems are as follows; first, the method is easy to implement and it can therefore be used to get an idea of the solution; second, the marker method, even when using a crude temporal integration technique (such as the first-order Euler algorithm) and a basic shape function, can be used as an initial guess for some more accurate iterative techniques.

The solution of integral equations using the marker method is more difficult and it requires further work.

Acknowledgements

This research was supported by Contract No. DE-AC02-76CH03073 and the Scientific Discovery through Advanced Computing (SciDAC) initiative (US Department of Energy).

References

[1] C.K. Birsdall, A.B. Langdon, Plasma Physics via Computer Simulations, McGraw-Hill, New York, 1985.
[2] J.M. Burgers, The Nonlinear Diffusion Equation: Asymptotic Solutions and Statistical Problems, Reidel, Boston, 1977.
[3] W. Chen, New RBF Collocation Schemes and Kernel RBFs with Applications, in: Lectures Notes in Computational Science and Engineering, vol. 26, Springer, Berlin, 2002.
[4] R. Courant, K. Friedrichs, H. Lewy, Math. Ann. 100 (1928) 32.
[5] A.F. Ghoniem, F.S. Sherman, J. Comp. Phys. 61 (1985) 1.
[6] R.W. Hockney, J.W. Eastwood, Computer Simulations using Particles, McGraw-Hill, New York, 1981.
[7] D.J. Korteweg, G. de Vries, Philos. Mag. 39 (1895) 422.
[8] J.L.V. Lewandowski, Phys. Plasmas 10 (2003) 3204.
[9] J.L.V. Lewandowski, J. Sci. Comput. 21 (2) (2004) 174.
[10] W.S. Press, S.A. Teukolsky, W.T. Vetterling, B.P. Flannery, Numerical Recipes in Fortran, Cambridge University Press, New York, 1992.
[11] P. Raviart, An analysis of particle methods, in: F. Brezzi (Ed.), Numerical Methods in Fluid Dynamics, Lecture Notes in Mathematics, vol. 1127, Springer, Berlin, 1985.